Journal of Loss Prevention in the Process Industries 65 (2020) 104099

Contents lists available at ScienceDirect

Journal of Loss Prevention in the Process Industries

journal homepage: http://www.elsevier.com/locate/jlp

Configuration predictions of large liquefied petroleum gas (LPG) pool fires using CFD method

Hang Yi [a], Yu Feng [a,**], Haejun Park [c], Qingsheng Wang [b,*]

[a] School of Chemical Engineering, Oklahoma State University, Stillwater, OK, 74078, USA
[b] Mary Kay O'Connor Process Safety Center, Artie McFerrin Department of Chemical Engineering, Texas A&M University, College Station, TX, 77843, USA
[c] Department of Fire Protection & Safety, Oklahoma State University, Stillwater, OK, 74078, USA

ARTICLE INFO

Keywords:
Liquefied petroleum gas (LPG)
Pool fire
Flame height
Flame tilt
Computational Fluid Dynamics (CFD)

ABSTRACT

Liquefied petroleum gas (LPG) has potential pool fire risks due to its flammability. The configuration of pool fires plays a significant role when applying the solid flame model or point source model to assess the risks from heat radiation. However, no existing correlations can precisely predict the configuration of large LPG (100% propane) pool fires. To enhance the fundamental understanding on how pool diameter and wind velocity can influence the configuration of large LPG pool fires, an experimentally validated Computational Fluid Dynamics (CFD) model is employed to simulate fires using different burning rate models. Fire temperature profiles, flame heights, and flame tilts predicted by the CFD model were compared with empirical models and experimental data. Accordingly, new correlations for flame height and flame tilt as functions of pool diameter D and wind velocity u_w have been developed. The comparisons demonstrate that the new correlations have the best overall accuracy in the prediction of flame height and tilt for large LPG pool fires under different conditions ($10\ m \leq D \leq 20\ m$, $0 \leq u_w \leq 3\ m{\cdot}s^{-1}$).

1. Introduction

To achieve the goal of clean cooking and heating by 2030, the demand for liquefied petroleum gas (LPG) as a low-pollution fuel is increasing rapidly (Kojima, 2011). Pool fire can be generated if there is an LPG leakage during transportation or at storage sites. Thus, understanding the characteristics, i.e., the radiation and configuration of LPG pool fire, are necessary for the effective control of potential fire risks. Pool fire is defined as the combustion of material evaporating from a layer which is formed by a liquid fuel pool (Van den Bosch and Weterings, 1997). The liquid fuel spreads out horizontally and forms turbulent, non-premixed, and diffusive flame (Vela et al., 2009). A large-scale LPG pool fire, i.e., beyond the experimental scale available for study in laboratory or largest field tests, could lead to severe consequences and losses with high flame temperature and heat flux to its surroundings. Thus, studying the pool fire configurations is essential, which will provide direct evidence to accurately predict the radiative heat flux and evaluate the induced risks to the ambient environment (Yi et al., 2019). Experiments have been conducted to investigate the flame height and wind effect on the flame distribution of LPG pool fires (Droste and Schoen, 1988; Hiroshi and Koseki, 2001; Johnson et al., 1980; Palazzi and Fabiano, 2012). However, they focused on small-scale fires with pool diameters less than 10 m, and large-scale LPG pool fires have not been well investigated by experiments due to the high costs, measurement difficulties, and safety considerations (Trouvé, 2008.; Vasanth et al., 2013). Nevertheless, there are many empirical or semi-empirical models and correlations developed based on experimental data for the flame height and tilt of small-scale pool fires (A.G.A, 1974; Bariha et al., 2017; Moorhouse, 1982; Sengupta, 2019; Steward, 1970; Thomas, 1963; Welker and Sliepcevich, 1966). These models may lead to significant errors when being applied to large-scale pool fires, which have been discussed in discussion part of this paper. So far, there are no specific correlations for flame height and tilt in large LPG (100% propane) pool fires with diameters larger than 10 m. Thus, more reliable and accurate correlations for flame height and tilt should be developed to enhance the fundamental understanding of the large LPG pool fire configurations.

Since experimental investigations are difficult for large-scale LPG pool fires, Computational Fluid Dynamics (CFD) models have been employed as an alternative time-saving and cost-effective tool based on first principles of physics and chemistry (Joshi et al., 2016; Wang et al., 2016, 2018; Yi et al., 2019). The CFD capability to accurately simulate

* Corresponding author.
** Corresponding author.
E-mail addresses: hang.yi@okstate.edu (H. Yi), yu.feng@okstate.edu (Y. Feng), qwang@tamu.edu (Q. Wang).

https://doi.org/10.1016/j.jlp.2020.104099
Received 27 January 2020; Received in revised form 11 March 2020; Accepted 11 March 2020
Available online 14 March 2020

Nomenclature

A	The pool area, m^2
c_p	Specific heat of air at constant pressure, $kJ{\cdot}kg^{-1}{\cdot}K^{-1}$
D	LPG pool diameter, m
F	A flame shape factor for radiation to the liquid
g	Acceleration of gravity, $m{\cdot}s^{-2}$
Fr	Froude number
ΔH_v	Heat of vaporization, $J{\cdot}kg^{-1}$
ΔH_C	Heat of combustion, $kJ{\cdot}kg^{-1}$
k	An extinction coefficient
k_1	Thermal conductivity, $W{\cdot}m^{-1}{\cdot}K^{-1}$
$k_1^{'}$	An opacity coefficient
$k_1^{'}$	Rate coefficient
k_2	Convective heat transfer coefficient, $W{\cdot}m^{-2}{\cdot}K^{-1}$
$\dot{m}$	Mass burning rate, $kg{\cdot}s^{-1}$
$\dot{m}^{''}$	Mass burning rate per unit area, $kg{\cdot}m^{-2}{\cdot}s^{-1}$
$\dot{m}_{\infty}^{''}$	Maximum mass burning rate per unit area, $kg{\cdot}m^{-2}{\cdot}s^{-1}$
$\dot{q}^{''}$	Heat flux, $W{\cdot}m^{-2}$
$\dot{Q}_C$	Rate of LPG heat release, kW
$\dot{Q}_C^*$	Non-dimensional rate of LPG heat release
r	The mass ratio of the stoichiometric air to the fuel
R	Regression rate, $mm{\cdot}min^{-1}$
R_{∞}	Radiation-dominant regression rate limit, $mm{\cdot}min^{-1}$
T_{∞}	Temperature far away from the LPG pool fire, K
T_B	Liquid surface temperature, K
T_F	Flame temperature, K
U	Gas velocity, $m{\cdot}s^{-1}$
u_{10}^*	Non-dimensional wind velocity at the height 10 m
u_w	Wind velocity, $m{\cdot}s^{-1}$
u^*	Non-dimensional wind velocity
v	Burning velocity defined by the liquid pool level decreases with time, $m{\cdot}s^{-1}$
W	The long-side length of a rectangular pool, m
α	A constant pressure expansion ratio for stoichiometric combustion
β	Mean beam length corrector
σ	Stefan-Boltzmann constant, 5.67×10^{-8} W $m^{-2}{\cdot}K^{-4}$
θ	Tilt angle, ◦
ϕ	Mole fraction composition of fuel-air mixture
ϕ_{st}	Stoichiometric fuel-air mixture mole fraction composition
ω	Inverse volumetric expansion ratio due to combustion
ν	Kinematic viscosity of air, $m^2{\cdot}s^{-1}$
ρ_{∞}	Far-end air density, $kg{\cdot}m^{-3}$
ρ_a	Ambient air density, $kg{\cdot}m^{-3}$
ρ_{LPG}	LPG density, $kg{\cdot}m^{-3}$
$\rho_{LPG}^{'}$	Density ratio between LPG and air
ρ_{LPGg}	Vaporized LPG density, $kg{\cdot}m^{-3}$
a	Ambient
C	Combustion
F	Flame
g	Gas
LPG	Liquefied petroleum gas
p	Pressure
st	Stoichiometric
v	Vaporization
w	Wind

pool fires has been proved by previous studies. The early CFD effort to simulate fire dynamics was done by Galea (1989), who used the field modeling approach to simulate enclosure fires. Sun et al. (2014) used Large Eddy Simulation (LES) to analyze the radiation from liquefied natural gas (LNG) pool fires and provided insight on determining the safe distance between LNG tanks and vaporizers. Vasanth et al. (2015) showed good agreements between experimental measurements and CFD simulation results in flame temperature, radiation, and burning rates of multiple pool fires situated at differing elevations. Chow et al. (2017) obtained flame height correlations, and thermal parameters in fire tornados using ANSYS Fluent validated *via* the comparison with experimental data. Therefore, it is feasible to employ CFD simulations to investigate the configuration properties of large LPG pool fires.

In this study, the characteristics of burning rate, flame height, and flame tilt of large LPG pool fires were investigated and compared using empirical models, correlations, and CFD simulations. Specifically, integrating the Re-Normalization Group (RNG) k-ε model, P-1 radiation model, and the non-premixed combustion model, the CFD model was developed in ANSYS Fluent 2019 R2 (ANSYS Inc., Canonsburg, PA) to study the configuration of large LPG pool fires with pool diameters between 10 m and 20 m in static and windy conditions ($0 \le u_w \le 3$ $m{\cdot}s^{-1}$). The burning rates, flame heights, and tilts of large LPG pool fires using different methods are compared with the experimental data obtained by Mudan (1984a). Subsequently, two new correlations for flame heights and one new correlation for flame tilts are proposed with better accuracy specifically for large-scale LPG pool fires.

2. Theory

In large LPG pool fires, the radiative heat flux can be influenced by many variables, such as the pool size, the fire configuration (*i.e.,* flame height and tilt), the duration of the fire, the distance to the ambient targets, and the characteristics of the targets exposed to the thermal radiation. The total radiative heat flux in a pool fire is determined by the burning rate, flame height, and flame tilt, which had significant impacts on radiation distributions when point source model and solid flame model are used to estimate the heat flux to surrounded targets. Therefore, when predicting the radiation to ambient human and constructions around large LPG pool fires, the above-mentioned variables should be considered comprehensively. The details are discussed in the following sections.

2.1. Burning rate models

The burning rate varies mainly with the pool fire size, and is also influenced by the ambient air velocity, *i.e.,* the wind speed (Johnson et al., 1980). In general, the burning rate $\dot{m}$ of a pool fire can be expressed as:

$$\dot{m} = \frac{\pi \dot{m}^{''} D^2}{4} \tag{1}$$

and

$$\dot{m}^{''} = \rho_{LPG} v \tag{2}$$

where $\dot{m}$, $\dot{m}^{''}$, and v are burning rates defined in mass per second, mass per unit area per second, and velocity, respectively (Drysdale, 2011).

Johnson et al. (1980) developed a correlation to describe the relationship between the burning rate v and pool diameter D based on the experimental data of small pool fires, which shows that the maximum burning rate v has been reached to 1.905×10^{-4} $m{\cdot}s^{-1}$ when the pool size is larger than 0.508 m.

Blinov and Khudiakov (1957) proposed that burning rates were determined dominantly by the heat flux from the fire plume to the liquid

pool surface. Based on such a hypothesis, the following correlation was proposed by Hottel (1959), i.e.,

$$\dot{q}'' = k_1 \frac{T_F - T_B}{D} + k_2 (T_F - T_B) + \sigma T_F^4 \cdot F\left(1 - e^{-k' D}\right) \tag{3}$$

It is worth mentioning that the first and second terms on the right-hand side of Eq. (3) represent conduction and convection, which can be neglected when the pool fire diameter is larger than 0.3 m (Drysdale, 2011; Zabetakis and Burgess, 1961). Being divided by the volumetric heat of vaporization $\rho_{LPG}\Delta H_v$ on both sides, Eq. (3) can be further simplified to

$$v = \frac{\sigma T_F^4 F}{\rho_{LPG}\Delta H_v}\left(1 - e^{-k' D}\right) \times 10^{-3} \tag{4}$$

To facilitate the calculation, the regression rate R (mm·min^{-1}) was introduced by Blinov and Khudiakov (1957). As a result, the LPG pool burning rate can be simplified to

$$\dot{m}'' = \frac{\rho_{LPG} R}{60} \times 10^{-3} \tag{5}$$

where the regression rate R can be given as:

$$R = R_\infty \left(1 - e^{-k_1' D}\right) \tag{6}$$

Zabetakis and Burgess (1961) recommended another equation to predict the burning rate $\dot{m}''$ of liquid pool fires of which the pool diameter is greater than 0.2 m in the static air:

$$\dot{m}'' = \dot{m}''_\infty \left(1 - e^{-k\beta D}\right) \tag{7}$$

For the liquid LPG (100% propane) used in Eq. (7), ρ_{LPG}, $\dot{m}''_\infty$, and $k\beta$ are considered as 585 kg·m^{-3}, 0.099 kg m^{-2}·s^{-1}, and 1.4 m^{-1} in this study, respectively (Babrauskas, 1983).

In order to calculate the thermal radiation of pool fires directly, Liu et al. (2009) used a simplified equation to calculate the burning rate v, i.e.,

$$v = \frac{\left(6.932 - 6.01^{\frac{-D}{1.31}}\right)}{6} \times 10^{-4} \tag{8}$$

Since the regression rate R for LPG (100% propane) is still not available and needs to be identified, the above-mentioned three models (Johnson et al., 1980; Liu et al., 2009; Zabetakis and Burgess, 1961) were employed to predict the burning rate of large LPG pool fires in this study, and all values have been converted to mass burning rate $\dot{m}$ shown in Fig. 3 using Eqs. (1) and (2).

2.2. Flame height models

The flame height is an important variable for the estimations of surface emissive power and radiation from large LPG pool fires to its surroundings when the point source model and solid flame model are employed. Many numerical models and correlations have been developed to predict the flame height for different hydrocarbon pool fires in the past decades, among which a dimensionless number H/D (Hurley et al., 2016) was often employed. The flame height model is usually proposed as a function of the Froude number Fr which is defined as (Drysdale, 2011):

$$Fr = \frac{U^2}{gD} \tag{9}$$

and

$$U = \frac{4\dot{Q}_C}{\pi \Delta H_C \rho_{LPG} D^2} \tag{10}$$

A dimensionless heat release rate $\dot{Q}_C^*$ was introduced to classify fire types and flame height (McCaffrey, 1995; Zukoski, 1995) expressed by

$$\dot{Q}_C^* = \frac{\dot{Q}_C}{\rho_\infty c_p T_\infty \sqrt{gD} D^2} \tag{11}$$

Based on Eq. (11), Thomas (1963) further developed a correlation for the mean visible height of turbulent diffusion flames in still air:

$$H \Big/ D = 42 \left(\frac{\dot{m}''}{\rho_a \sqrt{gD}}\right)^{0.61} \tag{12}$$

Steward (1970) developed a similar correlation with a dimensionless parameter of inverse volumetric expansion ratio due to combustion expressed by:

$$H \Big/ D = 14.73 \left(\frac{\omega\left(r + \frac{\omega}{\rho_{LPG}}\right)}{(1-\omega)^5}\right) \left(\frac{\dot{m}''}{\rho_a \sqrt{gD}}\right)^{0.4} \tag{13}$$

and

$$\rho'_{LPG} = \frac{\rho_{LPGg}}{\rho_a} \tag{14}$$

ω is determined using the following equation:

$$\omega = \frac{\phi - \phi_{st}}{\alpha(1 - \phi_{st})} \tag{15}$$

where α is equal to 8.0 for hydrocarbons (Tugnoli et al., 2013), ϕ is the mole fraction composition of the fuel-air mixture and ϕ_{st} is the stoichiometric mole fraction composition fraction for the fuel-air mixture.

Specifically, since the composition of LPG in the United States is pure propane (Hahn, 2019), the evaporated fuel cloud in this study can be considered as pure propane vapor. Therefore, parameter values for pure propane were used. For example, ω is equal to $\frac{1}{9}$ (Mannan, 2012), and r is equal to 15.6. Using Eqs. (13)–(15), a new correlation which focuses on the flame height of LPG pool fires is proposed as follows:

$$H \Big/ D = 46.24 \left(\frac{\dot{m}''}{\rho_a \sqrt{gD}}\right)^{0.4} \tag{16}$$

Based on previous correlations and experimental results (Heskestad, 1981 &1983b), Heskestad (1983a) has obtained the following correlation:

$$H \Big/ D = 15.6 \left(\frac{c_p T_\infty \dot{Q}_c^{\,2}}{g\rho_\infty^2 (\Delta H_c / r)^3 D^5}\right)^{1/5} - 1.02 \tag{17}$$

McCaffrey (1995) further simplified Eq. (17) in terms of $\dot{Q}_C^*$. Specifically, when $0.12 < \dot{Q}_C^* < 1.2 \times 10^4$, Eq. (17) can be rewritten as:

$$H / D = 3.7 \dot{Q}_C^{*\,2/5} - 1.02 \tag{18}$$

Besides, the presence of wind may also alter the visible length of flames when the wind velocity is large enough. The correlation developed by Thomas (1963) explicitly shows the wind effect on the wood crib flames:

$$H \Big/ D = 55 \left(\frac{\dot{m}''}{\rho_a \sqrt{gD}}\right)^{0.67} (u^*)^{-0.21} \tag{19}$$

where u^* is the nondimensionalized wind velocity defined by

$$u^* = u_w \left(\frac{g\dot{m}'' D}{\rho_{LPGg}}\right)^{-\frac{1}{3}} \tag{20}$$

Moorhouse (1982) conducted several large-scale experiments for

LNG pool fires. The crosswind and downwind were analyzed to determine the exact flame length, and the correlated flame height expressed by

$$H \Big/ D = 6.2 \left(\frac{\dot{m}''}{\rho_a \sqrt{gD}}\right)^{0.254} \left(u_{10}^*\right)^{-0.044} \tag{21}$$

In Eq. (19), u^* is treated to be equal to 1.0 when it is less than 1.0 (Mudan, 1984b). Since Eq. (21) is used to estimate LNG pool fires under the windy condition, the correlations for large LPG pool fires can be refined based on Eq. (21) by using CFD simulations.

In this study, Eqs. (12) and (13) and (16)–(18) were employed to predict the flame height in static ambient air for large LPG pool fires. Equations (19) and (21) are used to estimate flame heights with ambient winds. It should be noticed that Eq. (16) was originally developed in this study specifically for LPG (100% propane) pool fires. In contrast, other correlations mentioned above are for other hydrocarbon fuels, which might lead to errors to predict flame heights of LPG pool fires.

2.3. Flame tilt models

The ambient airflow dynamics might have a significant impact on the flame in outdoor environments, which may affect the fire behaviors tremendously. The tilt angle θ is often used to describe the effect of crosswinds on flame (Oka et al., 2003), which is defined by the angle between the centerline of the flame and the normal direction of the pool, i.e., the Y axis (see Fig. 1).

In order to have a better understanding of the wind effect on the flame height of LPG pool fires, Oka et al. (2003) proposed an equation to predict the flame tilt angle ($20^\circ \le \theta \le 80^\circ$) for rectangle-shaped pools as a function of multiple variables, i.e.,

$$tan\theta = \begin{cases} 2.73 F_r^{0.4} Q_c^{*-0.55} \left(\frac{W}{r^*}\right)^{-0.5}, & \left(0.05 < Q_c^* \le 0.38\right) \\ 2.73 F_r^{0.4} Q_c^{*-0.267} \left(\frac{W}{r^*}\right)^{-0.5}, & \left(0.38 < Q_c^* \le 12.8\right) \end{cases} \tag{22a,b}$$

where W is the long side length of a rectangular pool, and r^* is the equivalent radius of the pool fire which is defined by:

$$r^* = \sqrt{A/\pi} \tag{23}$$

For LPG pool fires in circular shapes, Eq. (22 a & b) (Oka et al., 2003) can be simplified as follows

$$tan\theta = \begin{cases} 2.18 F_r^{0.4} Q_c^{*-0.55}, & \left(0.05 < Q_c^* \le 0.38\right) \\ 2.18 F_r^{0.4} Q_c^{*-0.267}, & \left(0.38 < Q_c^* < 12.8\right) \end{cases} \tag{24a,b}$$

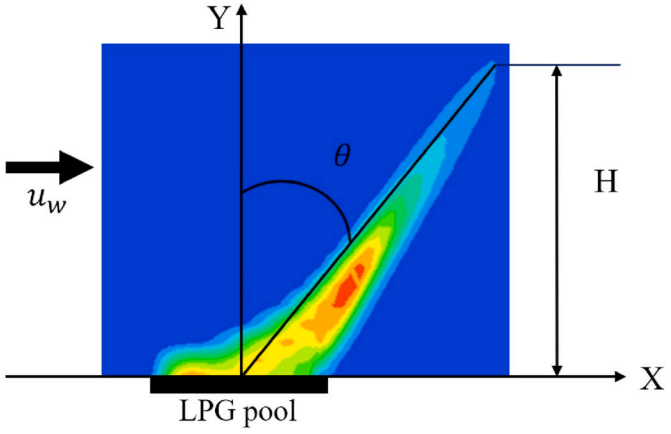

Fig. 1. Definition of the flame height H and flame tilt angle θ.

Additionally, an empirical correlation characterizing the wind speed effect on pool fire flame has been proposed by Rew et al. (1996):

$$\frac{\tan\theta}{\cos\theta} = 3.13 F_r^{0.2155} \tag{25}$$

Comparing different models including correlations mentioned by Mudan (1984b) with experimental data of pool fires, Fay (2006) developed another correlation for wind tilt which can be expressed as:

$$\sin\theta = \frac{F_r^2}{F_r^2 + 0.19} \tag{26}$$

Welker and Sliepcevich (1966) proposed another correlation based on small-scale liquid pool fire experiments, which is given as follows:

$$\frac{tan\theta}{cos\theta} = 3.3 \left(\frac{D u_w}{\nu}\right)^{0.07} \left(\frac{\rho_{LPG_g}}{\rho_a}\right)^{-0.6} F_r^{\,0.8} \tag{27}$$

Another correlation for flame tilt was derived based on the tests from wood cribs (Thomas, 1963):

$$cos\theta = 0.7 \left(\frac{u_w}{\left(g\dot{m}''/\rho_a\right)^{1/3}}\right)^{-0.49} \tag{28}$$

Moreover, A.G.A (1974) concluded a correlation using experimental data to determine the angle of tilt:

$$cos\theta = \begin{cases} 1, & \left(u^* < 1\right) \\ \frac{1}{\sqrt{u^*}}, & \left(u^* \ge 1\right) \end{cases} \tag{29a,b}$$

A global correlation was developed by Tang et al. (2015) to characterize the burning behaviors of acetone pool fire under crosswind ranging from 0 to 2.5 $m{\cdot}s^{-1}$ shown as follows:

$$tan\theta = 4.16 \left(\frac{\rho_a c_p (T_F - T_a) u_w^5}{\dot{m}'' D^2 \Delta H_c} \left(\frac{T_a}{g(T_F - T_a)}\right)^2\right)^{0.2} \tag{30}$$

More recently, Hu et al. (2013) used another correlation to describe the tilt angle for n-heptane and ethanol pool fires in terms of the ratio of the cross-flow air velocity and the uprising velocity of the buoyancy-induced flame:

$$tan\theta = 9.1 \left(\frac{\rho_a c_p (T_F - T_a) u_w^5}{\dot{m}'' D^2 \Delta H_c} \left(\frac{T_a}{g(T_F - T_a)}\right)^2\right)^{0.2} \tag{31}$$

2.4. Governing equations of the CFD model

The conservation laws of mass, energy, momentum, as well as constitutive equations of chemical kinetics, RNG k-ε turbulence model, P-1 radiation model, and non-premixed combustion model consist the closed equation system for the CFD simulations, which are documented in detail in previous publications (Yi et al., 2019).

3. Numerical method

3.1. Geometry and mesh

A 3-D computational domain for a large LPG pool fire at the center was constructed, with a pool diameter of 10.4 m (see Fig. 2). The O-Grid mesh was generated for the cylindrical flame region using ICEM CFD 2019 R2 (ANSYS Inc., Canonsburg, PA). In order to achieve the optimized balance between computational accuracy and efficiency, a mesh independence test was performed among four meshes with different element sizes (Yi et al., 2019). The final structured hexahedral mesh contains 3,694,764 cells. To eliminate the pool size effect, the meshes have been scaled with factors 1.240, 1.433 and 1.625 for the pools with 12.9 m, 14.9 m and 16.9 m in diameters, respectively.

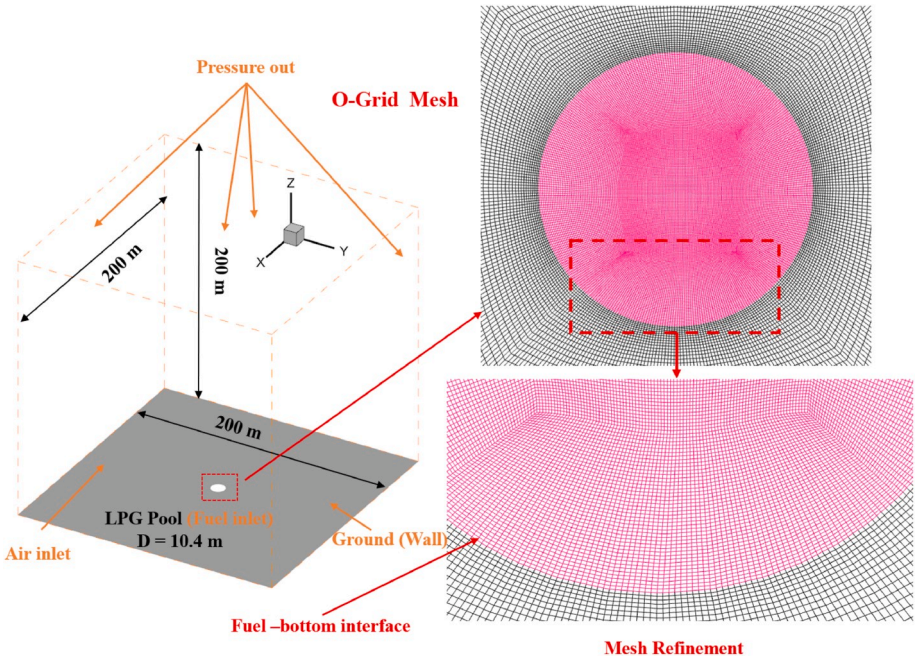

Fig. 2. Flow domain and the structured hexahedral final mesh for LPG pool fire simulations (D = 10.4 m and $\dot{m}$ = 8.406 kg·s^{-1}).

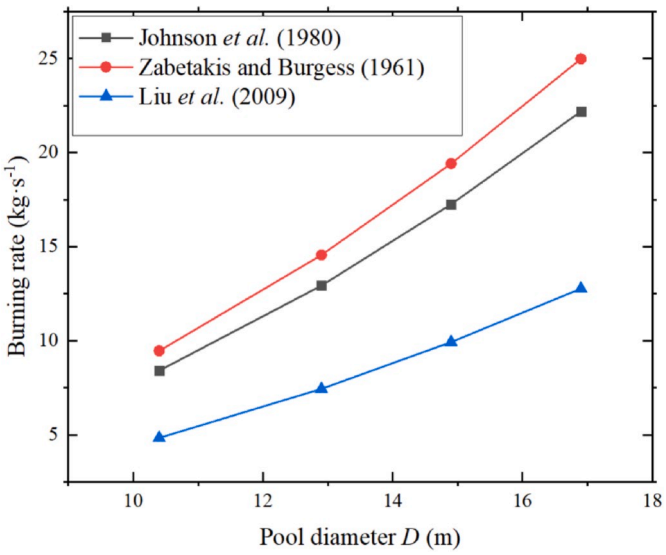

Fig. 3. Relationships between burning rates $\dot{m}$ and pool diameters (10.4 m ≤ D ≤ 16.9 m) using three different models in large LPG pool fires.

3.2. Numerical setup

A total of 19 CFD simulation cases were performed to study the configuration characteristics of large LPG pool fires. Specifically, three cases were used to seek for the best burning rare model as a function of pool diameter for large LPG pool fires, and another sixteen cases investigated how flame height and tilt can be influenced by the pool diameter (10 m ≤ D ≤ 20 m) and wind velocity (0 ≤ u_w ≤ 3.0 m·s^{-1}). The distinguished temperature for flames from the black smoke zone was considered as 800 K (Hägglund and Persson, 1976; Yi et al., 2019). The LPG pool fire simulations are considered steady-state in this study. A user-customized, commercial volume-finite based computer program, i.e., ANSYS Fluent 2019 R2 (ANSYS Inc., Canonsburg, PA) was employed to perform numerical solutions of the given governing equations (see Section 2.4) (Yi et al., 2019) with appropriate boundary conditions (see Table 1). Boundary conditions were determined based on empirical models and experimental measurements (Mudan, 1984a) shown in Table 1. Simulations were run on a local 64-bit Dell Precision Tower 7810 with 128 GB of RAM and dual 3.40 GHz processors. Second-order upwind schemes were adopted to discretize the governing equations of mass, momentum, turbulent kinetic energy, turbulent dissipation rate, energy, mean mixture fraction, and mixture fraction variance. The coupled scheme was employed for pressure-velocity coupling, and the least-squares cell-based schemes were applied for spatial discretizations. 1.0E-6 was assigned as the convergence criteria for energy and P1, and 1.0E-3 for the rest equations.

4. Results and discussion

4.1. Comparisons of predicted flame heights to find the best burning rate model

Although the experimental data are well documented in a benchmark research report for LPG pool fires with different diameters (Mudan, 1984a), the burning time of these pool fire in the experiments was not recorded precisely. Due to lack of the burning duration data in the experiments, it is impossible to estimate the average mass burning rate accurately with the only given information of total LPG burned mass. Since the burning rate is a key boundary condition for CFD simulations, which determines the accuracy of flame height and tilt angle predictions for large LPG pool fires, three widely used burning rate models were employed (see Section 2.1 and Fig. 3) in CFD simulations. To find the most accurate burning rate model for large LPG pool fire simulations, comparisons of the predicted flame heights using different burning models has been done with the benchmark experimental measurements (Mudan, 1984a) (see Fig. 4 (a)–(c)).

Specifically, according to the previous study (Yi et al., 2019), flame height is majorly determined by the burning rates in static air for large LPG pool fires. Therefore, CFD simulations for the pool fire with D = 16.9 m in static air were performed using the three burning rate models (see Fig. 3). The configurations of the flames colored by temperature are shown in Fig. 4. Fig. 4 (a)–(c) show three different flame heights, i.e., 41.52 m, 66.21 m, and 72.47 m, corresponding to three burning rate models. Experimental measurements (Mudan, 1984a) show that the

Table 1
Boundary conditions employed in CFD simulations for large LPG pool fires.

	Pool diameter (m)	Ambient temperature (K)	Average mass burning rate $\dot{m}$ (kg•s^{-1})	Faces					
				X+	X-	Y+	Y-	Z+	Z-
				Air velocity u_w (m•s^{-1})	Pressure outlet				
Finding the best burning rate	16.9	312	14.972 22.196 24.986	0	Gauge pressure = 0				Non-slip wall
Flame heights and tilts simulations	10.4	306	8.406	0 0.5 2.5 3					
	12.9	309	12.932	0 0.5 2.5 3					
	14.9	306	17.254	0 0.5 2.5 3					
	16.9	312	22.196	0 0.5 2.5 3					

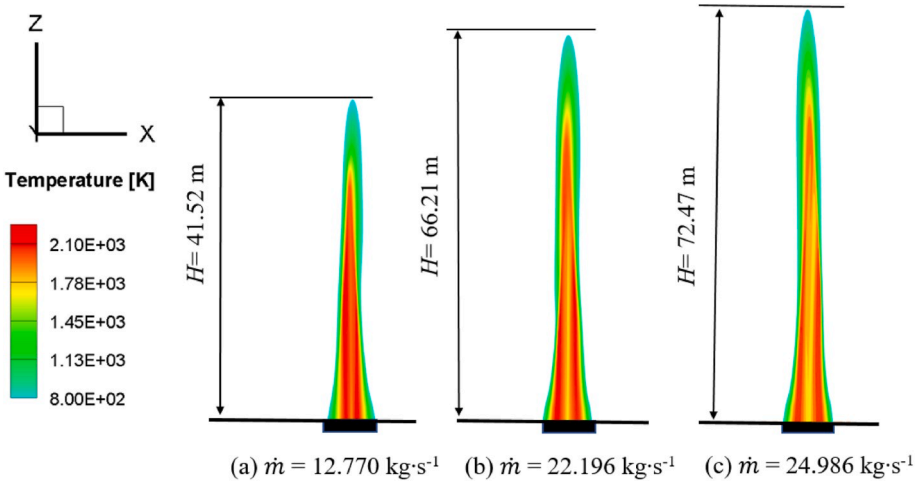

Fig. 4. Predicted flame configurations of large LPG pool fires (D = 16.9 m, u_w = 0) colored by temperature (K) using three different burning rates: (a) $\dot{m}$ = 12.770 kg·s^{-1} (Liu et al., 2009), (b) $\dot{m}$ = 22.196 kg·s^{-1} (Johnson et al., 1980), (c) $\dot{m}$ = 24.986 kg·s^{-1} (Zabetakis and Burgess, 1961).

flame height for the same large LPG pool fire with the diameter 16.9 m is 54 m. Thus, it can be found that the flame height predicted in Fig. 4 (b) using Johnson's burning rate model (Johnson et al., 1980) provides the best match to experiments. The flame height with burning rate 12.770 kg·s^{-1} is smaller than a regular LPG pool fire (Mudan, 1984a), which implies that the burning rate in a regular LPG pool fire should be larger than 12.770 kg·s^{-1}. The temperature profile is more likely a jet fire rather than a pool fire when the burning rate is 24.986 kg·s^{-1} because the flame height is 34% higher than a normal LPG pool fire (Mudan, 1984a & 1984b). Therefore, to reduce the relative errors between the CFD simulations and experiments, the burning rate model proposed by Johnson et al. (1980) was selected as the boundary conditions values in CFD simulations to predict the flame heights and tilts in large LPG pool fires. Moreover, the parametric analysis of between flame height and pool diameter (see Figs. 5–9 and Table 2 in Section 4.2) also indicate that Johnson's burning rate model is more precise and reliable in flame height predictions in large LPG pool fires compared with experimental data.

4.2. Flame height vs. pool diameter and wind velocity

According to the experimental report (Mudan, 1984a), the flame heights were 54.9 m, 51.9 m and 54.4 m in the LPG pool fires with the corresponding diameters of 12.9 m, 14.9 m and 16.9 m under different wind velocities ($0 \leq u_w \leq 3$ m·s^{-1}), respectively. To obtain the flame heights with different pool diameters and wind velocities, the flame heights covered by the temperature magnitude with corresponded pool sizes (10.4 m $\leq D \leq$ 16.9 m) under the air velocity from 0 to 3 m·s^{-1} have been simulated using the CFD model and visualized in Figs. 5–8. Table 2 also quantitatively summarize how the flame height varies with the change of pool diameter at different wind velocity. It can be found that the flame height increases gradually as the burning rate grows up under the same air condition. These phenomena can be explained that the larger burning rate would generate more LPG vapor by the vaporization heat from the fire plume, and eventually form higher flames during the combustion process. Figs. 5–9 indicate that the flame height decreases with the increase in wind velocity, because higher wind velocity will enhance the vaporization of fuel gases and the tilt angle of the flame,

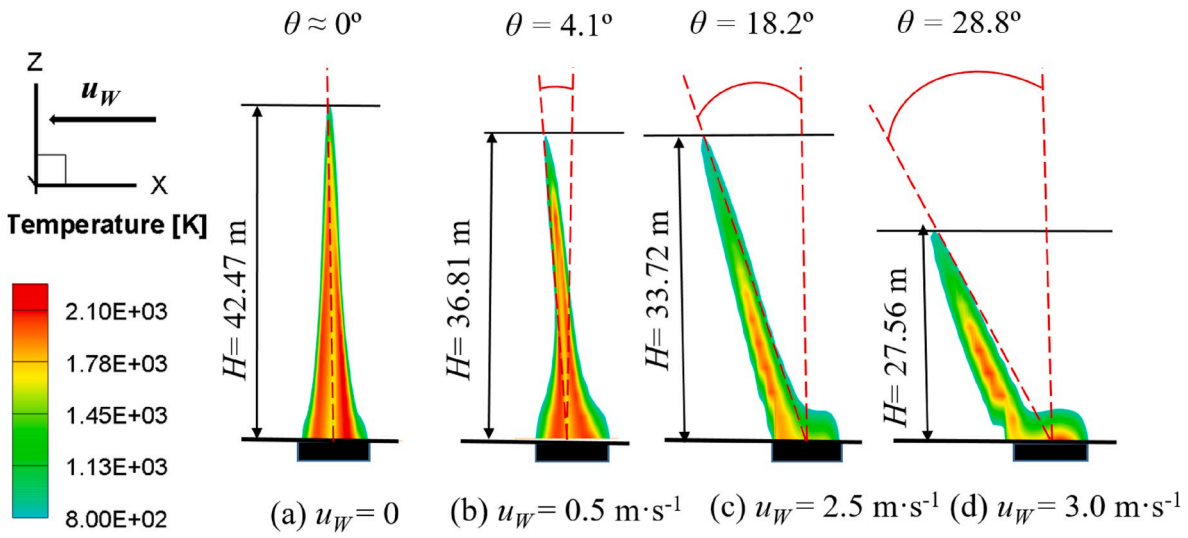

Fig. 5. Temperature (K) profiles of large LPG pool fires (D = 10.4 m) with different wind velocities: (a) u_w = 0, (b) u_w = 0.5 m·s^{-1}, (c) u_w = 2.5 m·s^{-1}, (d) u_w = 3 m·s^{-1}.

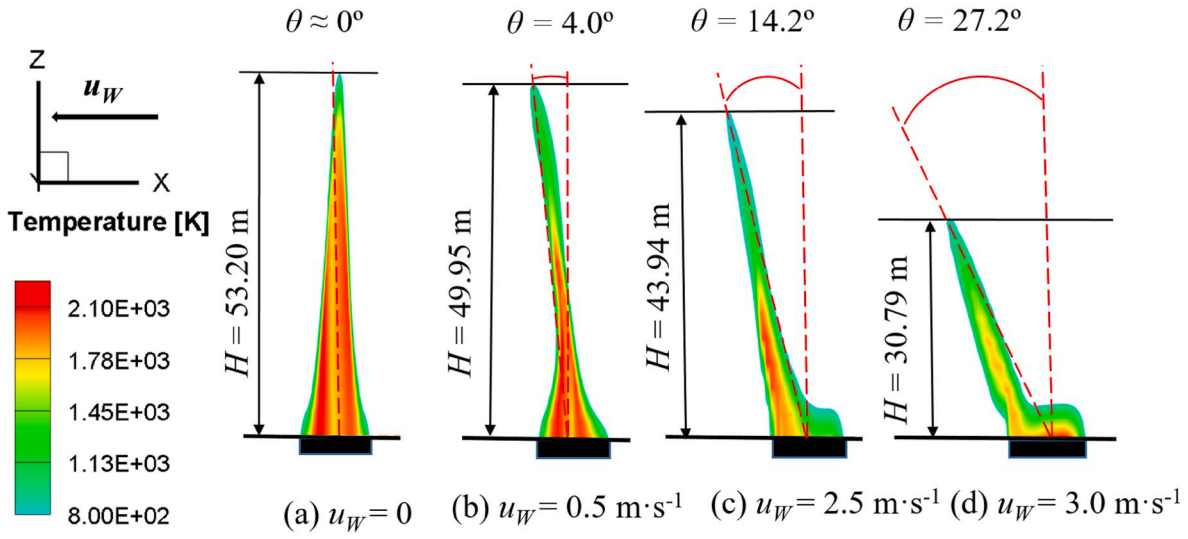

Fig. 6. Temperature (K) profiles of large LPG pool fires (D = 12.9 m) with different wind velocities: (a) u_w = 0, (b) u_w = 0.5 m·s^{-1}, (c) u_w = 2.5 m·s^{-1}, (d) u_w = 3 m·s^{-1}.

resulting in the flame axis more leaned towards the horizontal direction.

The comparisons of flame heights using empirical models, correlations, the only available experimental data (Mudan, 1984a), and the CFD simulations in this study are shown in Fig. 9 (a)–(d). Equations (12) and (16)–(18) have been used to estimate the flame height in the still air, which are shown in Fig. 9 (a)–(d). Compared with the flame heights predicted via the experimentally optimized and validated CFD model (see Section 4.1) as well as the experimental data, Eqs. (12), (17) and (18) underestimate the flame heights with noticeable errors. The deviations are due to the fact that Eqs. (12), (17) and (18) were developed specifically for small pool fires or other hydrocarbon pool fires, which are not appropriate to be employed to predict the large LPG pool fires. In contrast, Eq. (16) can predict the flame height of large LPG pool fires in the still air with much smaller deviations (see Fig. 9 (a)–(d)), which suggests that specific correlations should be developed for corresponded specific hydrocarbon fuels if more accurate values need to be obtained, because different hydrocarbon fuels has corresponded combustion parameter values, i.e., stoichiometric composition mole fraction ϕ_{st} and inverse volumetric expansion ratio due to combustion ω. These parameters have significant impacts on flame height prediction using Eq. (16) for LPG pool fires.

Furthermore, the wind velocity plays a significant role in the flame height which can be observed from Figs. 8 and 9. Flame height comparisons between the CFD simulations, experiments, and empirical models (see Eqs. (19) and (21)) have also been done for large LPG pool fires with different ambient wind velocities (see Fig. 9 (a)–(d)). It can be found that the flame height decreases as the wind velocity increases, which is due to the enhanced convection effect on vaporized fuel towards the horizontal direction compared with the vertical direction (also see Figs. 5–8). It is worth mentioning that the experimental data for the pool fire with D = 12.9 m and u^* = 1.35 (u_w = 3 m·s^{-1}) (see Fig. 9 (b)) does not agree well with the CFD simulation results and other empirical models, which may be induced by the experimental measurement errors. Additionally, CFD simulations (see the slopes in Fig. 9 (a)–(d)) show that the flame height decreases faster when u_w is between 2.5 m·s^{-1} and 3.0 m·s^{-1} than the cases when u_w is between 0 and 2.5 m·s^{-1}. Such trends may due to that the air velocity larger than 2.5 m·s^{-1} in the horizontal direction has a tremendous impact on the movement

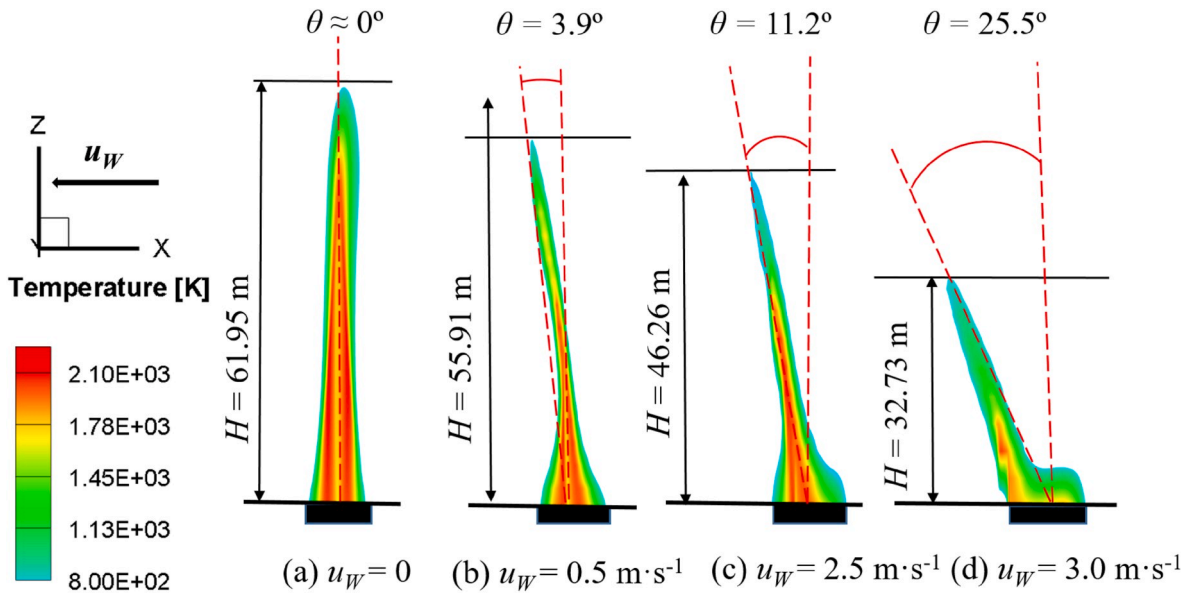

Fig. 7. Temperature (K) profiles of large LPG pool fires (D = 14.9 m) with different wind velocities: (a) u_w = 0, (b) u_w = 0.5 m·s^{-1}, (c) u_w = 2.5 m·s^{-1}, (d) u_w = 3 m·s^{-1}.

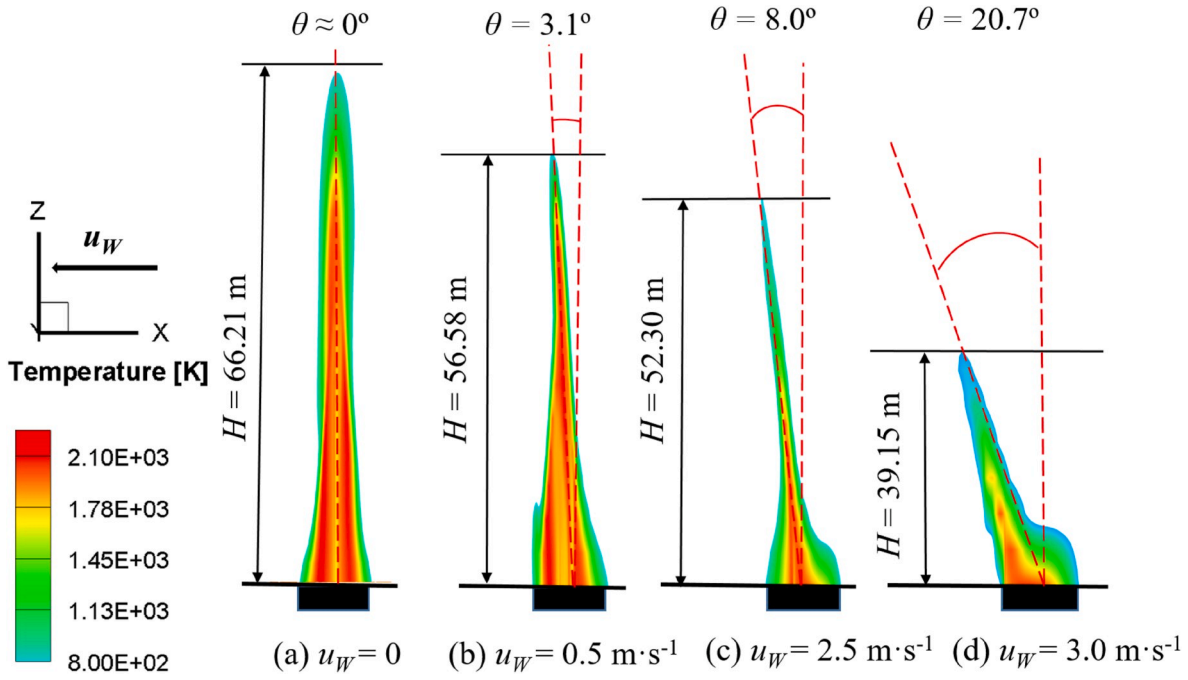

Fig. 8. Temperature (K) profiles of large LPG pool fires (D = 16.9 m) with different wind velocities: (a) u_w = 0, (b) u_w = 0.5 m·s^{-1}, (c) u_w = 2.5 m·s^{-1}, (d) u_w = 3 m·s^{-1}.

behavior of vaporized fuel gases in the vertical direction. While further investigation is needed in the near future. Based on the CFD simulation results shown in Fig. 9 (a)–(d), a new correlation is proposed to facilitate the estimation of flame heights for large LPG pool fires in engineering applications. Specifically for the LPG in the U.S., i.e., 100% propane (Hahn, 2019), the form of the new correlation is developed based on an existing paper (Thomas, 1963), which is given as follows:

$$H/D = 90\left(\dot{m}''/\rho_a\sqrt{gD}\right)^{0.67}(u^*)^{-0.21},\ \left(0 < u_w \le 2.5\,m\cdot s^{-1},\ 10\,m \le D \le 20\,m\right) \tag{32}$$

where u^* is a non-dimensional air velocity which is defined by Eq. (20).

Equation (32) provides more precise predictions for flame heights in the air velocity ($0 < u_w \le 2.5$ m·s^{-1}) compared with empirical correlations shown in Fig. 9 (a)–(d). It is worth mentioning that Eq. (32) is only available for pure propane. For other LPG compositions, Eq. (32) need to be further revised.

4.3. Flame tilt angle vs. pool diameter and wind velocity

Figures 5–8 show the flame tilt behaviors that are obtained by CFD simulations for large LPG pool fires with different diameters (10.4 m ≤ D ≤ 16.9 m) and wind velocity ($0 \le u_w \le 3$ m·s^{-1}). In addition, Table 3 quantitatively summarizes how the flame tilt angle varies with the

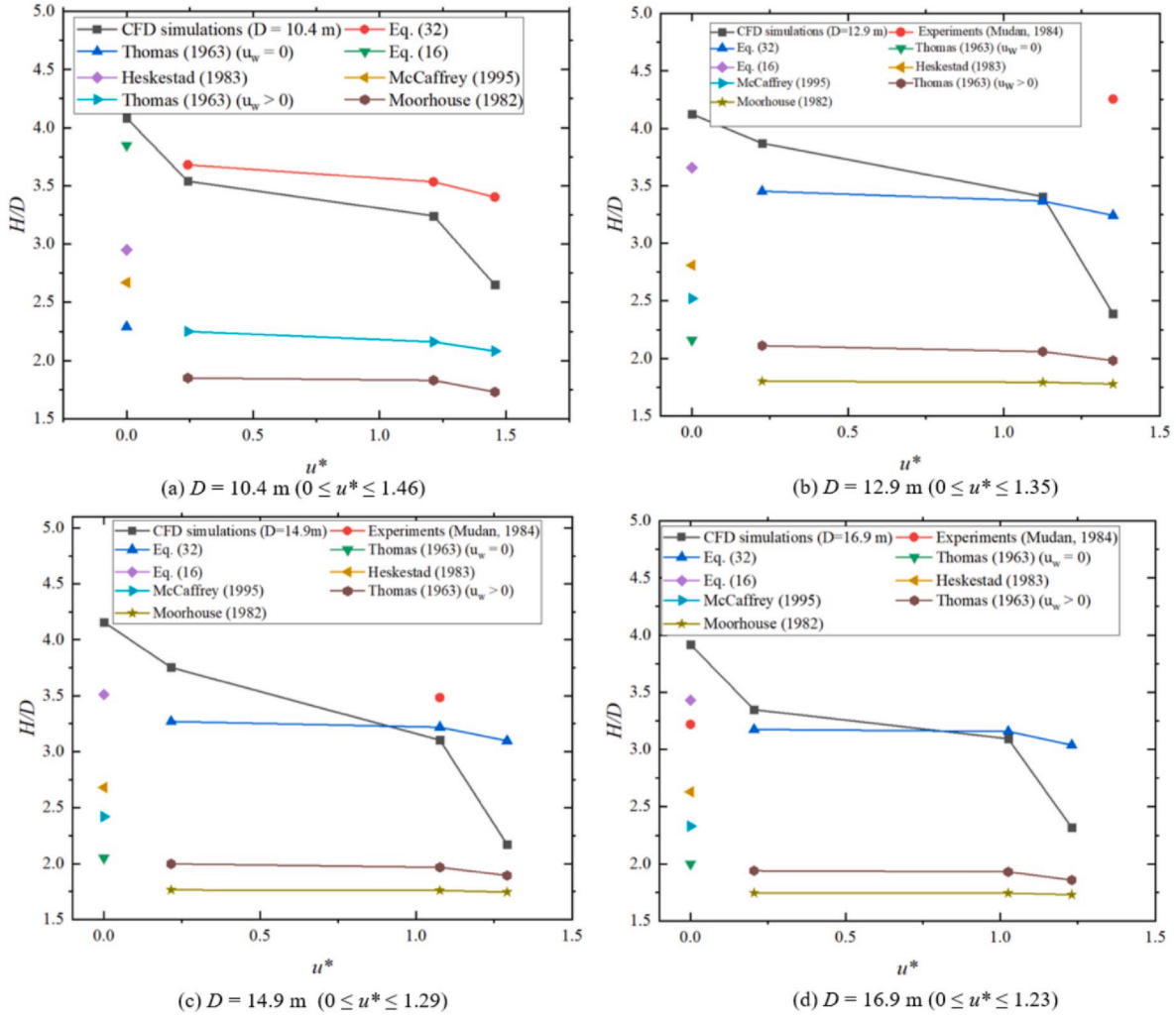

Fig. 9. Relationships between the nondimensionalized flame height H/D and nondimensionalized air velocity u^* with different pool diameters: (a) $D = 10.4$ m ($0 \leq u^* \leq 1.46$), (b) $D = 12.9$ m ($0 < u^* \leq 1.35$), (c) $D = 14.9$ m ($0 < u^* \leq 1.23$), (d) $D = 16.9$ m ($0 < u^* \leq 1.29$).

Table 2
Flame heights (m) for pool fires with different pool diameters (m) and wind velocities (m·s^{-1}).

	$D = 10.4$	$D = 12.9$	$D = 14.9$	$D = 16.9$
$u_w = 0.0$	42.47	36.81	33.72	27.56
$u_w = 0.5$	53.20	49.95	43.94	30.79
$u_w = 2.5$	61.95	55.91	46.26	32.73
$u_w = 3.0$	66.21	56.58	52.30	39.15

Table 3
Flame tilt angles for pool fires with different pool diameters (m) and wind velocities (m·s^{-1}).

	$D = 10.4$	$D = 12.9$	$D = 14.9$	$D = 16.9$
$u_w = 0.0$	0°	0°	0°	0°
$u_w = 0.5$	4.1°	4.0°	3.9°	3.1°
$u_w = 2.5$	18.2°	14.2°	11.2°	8.0°
$u_w = 3.0$	28.8°	27.2°	25.5°	20.7°

change of pool diameter at different wind velocity. It can be observed from Figs. 5–8 that the wind velocity also has a significant effect on the flame tilt angle due to the enhanced horizontal convection of the evaporated fuel. Indeed, the fire plume will lean downwind, and higher wind velocity will lead to a larger tilt angle at the same burning rate. Also, higher wind velocity will cause a more significant impact on the fire shape which is highly consistent with the high-concentration region of the evaporated LPG. Among all CFD simulation results, the maximum tilt angle appears at the pool fire with $D = 10.4$ m and $u_w = 3.0$ m·s^{-1}. It indicates that pool fire with a larger diameter will be less sensitive to the wind velocity. Indeed, larger pool diameter of the LPG pool fire indicates a higher burning rate $\dot{m}$ (see Fig. 3), so that the wind velocity effect will become relatively less important on evaporated fuel plume.

To obtain the effects of wind velocity on flame tilt angle for large LPG pool fires, the results from CFD simulations, empirical models, correlations, and experiments (Mudan, 1984a) have been analyzed and compared in Fig. 10 (a)–(d). The observation from Fig. 10 (a)–(d) also shows that the tilt angle increases with the increase of wind velocity. Compared with the CFD results, Eqs. (25), (28) and (31) overestimate the wind effects on the tilt angle of large LPG pool fires with the diameters from 10.4 to 16.9 m. It is also interesting to find that Eq. (25) predicts a trend that the slope is smaller in the air velocity (0.5 m·s^{-1} ≤ u_w ≤ 2.5 m·s^{-1}) than the corresponding value with the air wind from 0 to 0.5 m·s^{-1} (see Fig. 10 (a)–(d)), which is different from other empirical correlations and CFD simulations. The reason for this phenomenon needs further study. In contrast, Eq. (26) underestimates the wind effects on the tilt angle when comparing with other models and correlations. Therefore, the Froude number Fr and other parameters in Eq. (26) need to be correlated further when it is employed to investigate air effects on large LPG pool fires. In Fig. 10 (a)–(d), CFD simulations show that the

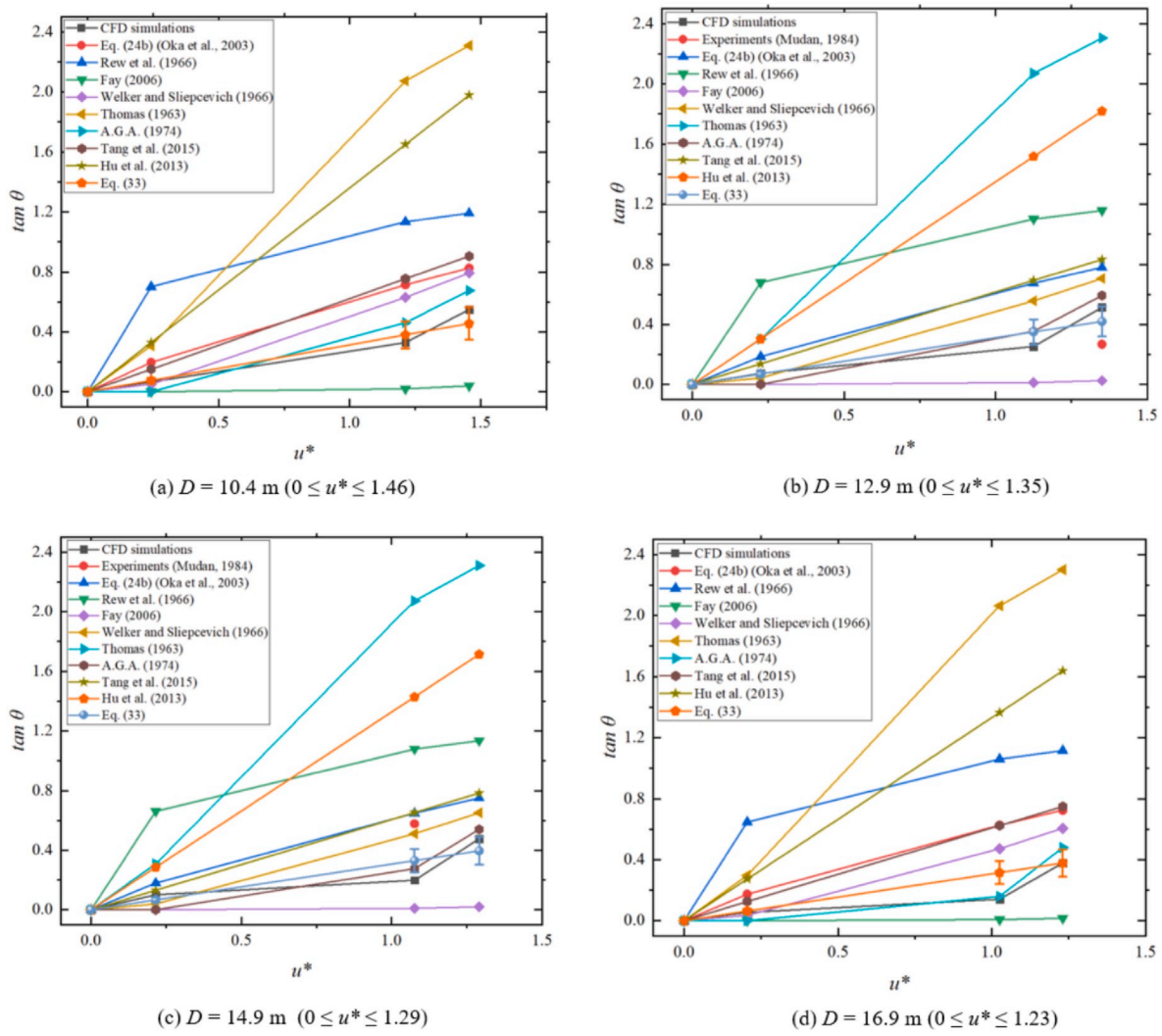

Fig. 10. Relationships between nondimensionalized flame tilt tan θ and nondimensionalized wind velocity u^* with different pool diameters: (a) $D = 10.4$ m ($0 \le u^* \le 1.46$), (b) $D = 12.9$ m ($0 \le u^* \le 1.35$), (c) $D = 14.9$ m ($0 \le u^* \le 1.23$), (d) $D = 16.9$ m ($0 \le u^* \le 1.29$).

flame tilt angle increases increase in wind velocity from 0 to 3 m·s^{-1} and matches experimental results better than other empirical correlations. Subsequently, Eq. (27) shows best agreements with CFD simulations with the air velocity u^* from 0 to 0.5 and Eq. 29 (b) matches the CFD simulations best when wind velocity u^* higher than 0.5 among all empirical correlations. Furthermore, according the correlations developed by Tang et al. (2015) for acetone pool fires and Hu et al. (2013) for the n-heptane and ethanol pool fires, an available correlation for flame tilt angle in large LPG pool fires (10 m $\le D \le$ 20 m) was proposed in a similar way based on results from the empirical correlations and simulations expressed by:

$$tan\theta = (2.1 \pm 0.4)\left(\frac{\rho_a c_p (T_F - T_a) u_w^5}{\dot{m}'' D^2 \Delta H_c}\left(\frac{T_a}{g(T_F - T_a)}\right)^2\right)^{0.2}, \quad (10\ \text{m} \le D \le 20\ \text{m}, 0 \le u_w \le 3\ \text{m} \cdot \text{s}^{-1}) \tag{33}$$

Figure 10 (a)–(d) show that the new proposed correlation Eq. (33) provides better predictions of flame tilt angles compared with CFD results than other empirical models for large LPG pool fires with the diameters (10 m $\le D \le$ 20 m).

5. Conclusions

In this study, numerical simulations were performed using an experimentally validated CFD model to simulate large LPG (100% propane) pool fires and predict the fire configuration characteristics including flame height and flame tilt. The impacts of pool diameter and wind velocity on the fire configuration characteristics were investigated. Based on the CFD results and the parametric analysis, new correlations are proposed to provide more accurate estimations of flame height and tilt specifically for large LPG pool fires. Quantitative conclusions are listed as follows:

- The selection of burning rate model can significantly influence the accuracy of flame height predictions using the CFD model. Johnson's

burning rate model is the best model among the three burning rate models employed in this study.
- Higher horizontal wind velocity will lead to stronger convection effect in the horizontal direction. As a result, it will reduce the flame height and increase the flame tilt angle.
- The configuration of LPG pool fires with larger diameters will be less sensitive to the ambient wind velocity.
- The new correlations proposed in this study provide more accurate predictions of the flame height and tilt angle than any existing empirical models. The two correlations will facilitate engineers and scientists when estimating the flame configurations for large LPG pool fires with pool diameters between 10 m and 20 m, and ambient wind velocity between 0 and 3 $m \cdot s^{-1}$.

With the enhanced fundamental understandings and the new proposed correlations of flame height and tilt, the CFD tool developed in this paper can be further employed to facilitate the precise risk assessment for large LPG pool fires in a time-saving and cost-effective manner.

Declaration of competing interest

The authors declare that they have no known competing financial interests or personal relationships that could have appeared to influence the work reported in this paper.

CRediT authorship contribution statement

Hang Yi: Methodology, Data curation, Writing - original draft. **Yu Feng:** Visualization, Methodology, Supervision, Writing - review & editing. **Haejun Park:** Validation. **Qingsheng Wang:** Conceptualization, Funding acquisition, Project administration, Supervision, Writing - review & editing.

Acknowledgments

The research was partially sponsored by the Fire Protection Research Foundation, United States. The use of ANSYS software (Canonsburg, PA) as part of the ANSYS-CBBL academic partnership agreement is gratefully acknowledged (Dr. Thierry Marchal, Global Industry Director). Some of the computing for this project was performed at the OSU High-Performance Computing Center at Oklahoma State University (Dr. Dana Brunson, Director and Dr. Evan Linde, Research Cyberinfrastructure Analyst).

Appendix A. : Supplementary data

Supplementary data to this article can be found online at https://doi.org/10.1016/j.jlp.2020.104099.

References

AGA, 1974. LNG Safety Research Program. Ameican Gas Association.
Babrauskas, V., 1983. Estimating large pool fire burning rates. Fire Technol. 19, 251–261.
Bariha, N., Srivastava Vimal, C., Mishra Indra, M., 2017. Theoretical and experimental studies on hazard analysis of LPG/LNG release: a review. Rev. Chem. Eng. 387–482.
Blinov, V.I., Khudiakov, G.N., 1957. Certain laws governing the diffusive burning of liquids. Academiia Nauk. SSR Doklady 113, 1094–1098.
Chow, W.K., Dang, J.F., Gao, Y., Chow, C.L., 2017. Dependence of flame height of internal fire whirl in a vertical shaft on fuel burning rate in pool fire. Appl. Therm. Eng. 121, 712–720.
Droste, B., Schoen, W., 1988. Full scale fire tests with unprotected and thermal insulated LPG storage tanks. J. Hazard Mater. 20, 41–53.
Drysdale, D., 2011. An Introduction to Fire Dynamics, third ed. John Wiley & Sons, NY.
Fay, J.A., 2006. Model of large pool fires. J. Hazard Mater. 136, 219–232.
Galea, E., 1989. On the field modelling approach to the simulation of enclosure fires. J. Fire Protect. Eng. 1, 11–22.
Hägglund, B., Persson, L., 1976. The Heat Radiation from Petroleum Fires. Forsvarets Forskningsanstalt, Stockholm.
Hahn, E., 2019. LPG Gas Mixture of Propane & Butane: Which Gas Is Present. LPG.
Heskestad, G., 1981. Peak gas velocities and flame heights of buoyancy-controlled turbulent diffusion flames. Symp. (Int.) Comb. 18, 951–960.
Heskestad, G., 1983a. Luminous heights of turbulent diffusion flames. Fire Saf. J. 5, 103–108.
Heskestad, G., 1983b. Virtual origins of fire plumes. Fire Saf. J. 5, 109–114.
Hiroshi, K., Koseki, H., 2001. Large scale pool fires: results of recent experiments. In: Fire Safety Science Proceedings of 6th International Symposium, pp. 71–88.
Hottel, H.C., 1959. Review: certain laws governing the diffusive burning of liquids by Blinov and Khudiakov(1957). Fire Res. Abst. Rev. 1, 41.
Hu, L., Liu, S., de Ris, J.L., Wu, L., 2013. A new mathematical quantification of wind-blown flame tilt angle of hydrocarbon pool fires with a new global correlation model. Fuel 106, 730–736.
Hurley, M.J., Gottuk, D.T., Hall Jr., J.R., Harada, K., Kuligowski, E.D., Puchovsky, M., Torero, J.L., Watts Jr., J.M., Wieczorek, C.J., 2016. SFPE Handbook of Fire Protection Engineering.
Johnson, D.W., Martinsen, W.E., Cavin, W.D., Chilton, P.D., Lawson, H.P., Welker, J.R., 1980. Control and Extinguishment of LPG Fires. Final Report. Applied Technology Corp., Norman, OK.
Joshi, P., Bikkina, P., Wang, Q., 2016. Consequence analysis of accidental release of supercritical carbon dioxide from high pressure pipelines. Int. J. Greenh. Gas Con. 55, 166–176.
Kojima, M., 2011. The Role of Liquefied Petroleum Gas in Reducing Energy Poverty, Extractive Industries and Development Series #25. World Bank, Washington, DC.
Liu, B., Liang, D., Huang, Y., 2009. Calculation and Simulation of Thermal Radiation of Pool Fire, vol. 9. Safety Health & Environment, pp. 36–38.
Mannan, M.S., 2012. Lees' Loss Prevention in the Process Industries, Volumes 1-3 - Hazard Identification, Assessment and Control. Elsevier.
McCaffrey, B., 1995. "Flame Height," SFPE Handbook of Fire Protection Engineering. National Fire Protection Association; Society of Fire Protection Engineers, Quincy, Mass.
Moorhouse, J., 1982. Scaling Criteria for Pool Fires Derived from Large Scale Experiments. British Gas Corporation, Solihull, England.
Mudan, K.S., 1984a. Hydrocarbon Pool and Vapour Fire Data Analysis.
Mudan, K.S., 1984b. Thermal radiation hazards from hydrocarbon pool fires. Prog. Energy Combust. Sci. 10, 59–80.
Oka, Y., Sugawa, O., Imamura, T., Matsubara, Y., 2003. Effect of cross-winds to apparent flame height and tilt angle from several kinds of fire source. Fire Saf. Sci. 7, 915–926.
Palazzi, E., Fabiano, B., 2012. Analytical modelling of hydrocarbon pool fires: conservative evaluation of flame temperature and thermal power. Process Saf. Environ. Protect. 90, 121–128.
Rew, P.J., Hulbert, W.G., Deaves, D.M., 1996. Development of pool fire thermal radiation model. In: HSE, W.S. (Ed.), Atkins Safety and Reliability. HSE Books, United Kingdom.
Sengupta, A., 2019. Optimal safe layout of fuel storage tanks exposed to pool fire: one dimensional deterministic modelling approach. Fire Technol. 55, 1771–1799.
Steward, F.R., 1970. Prediction of the height of turbulent diffusion buoyant flames. Combust. Sci. Technol. 2, 203–212.
Sun, B., Guo, K., Pareek, V.K., 2014. Computational fluid dynamics simulation of LNG pool fire radiation for hazard analysis. J. Loss Prev. Process. Ind. 29, 92–102.
Tang, F., Li, L.J., Zhu, K.J., Qiu, Z.W., Tao, C.F., 2015. Experimental study and global correlation on burning rates and flame tilt characteristics of acetone pool fires under cross air flow. Int. J. Heat Mass Tran. 87, 369–375.
Thomas, P.H., 1963. The size of flames from natural fires. In: 9th International Combustion Symposium, pp. 844–859.
Trouvé, A., 2008. CFD modeling of large-scale pool fires. In: The Second International Energy 2030 Conference, Abu Dhabi, U.A.E.
Tugnoli, A., Salzano, E., Di Benedetto, A., Russo, P., Cozzani, V., 2013. Analysis of the flash-fire scenario in the Viareggio accident. Chem. Eng. 32, 403–408.
Van den Bosch, C.J.H., Weterings, R.A.P.M., 1997. Methods for the Calculation of Physical Effects: Due to Releases of Hazardous Materials (Liquids and Gases), 'Yellow Book. CPR 14E. Sdu Uitgevers, The Hague.
Vasanth, S., Tauseef, S.M., Abbasi, T., Abbasi, S.A., 2013. Assessment of four turbulence models in simulation of large-scale pool fires in the presence of wind using computational fluid dynamics (CFD). J. Loss Prev. Process. Ind. 26, 1071–1084.
Vasanth, S., Tauseef, S.M., Abbasi, T., Abbasi, S.A., 2015. CFD simulation of pool fires situated at differing elevation. Process Saf. Environ. Protect. 94, 89–95.
Vela, I., Chun, H., Mishra, K.B., Gawlowski, M., Sudhoff, P., Rudolph, M., Wehrstedt, K. D., Schönbucher, A., 2009. Vorhersage der thermischen Strahlung großer Kohlenwasserstoff- und Peroxid-Poolfeuer mit CFD Simulation. Forsch. Im. Ingenieurwes. 73, 87–97.
Wang, W., He, T., Huang, W., Shen, R., Wang, Q., 2018. Optimization of switch modes of fully enclosed platform screen doors during emergency platform fires in underground metro station. Tunn. Undergr. Space Technol. 81, 277–288.
Wang, Z., Wang, W., Wang, Q., 2016. Optimization of water mist droplet size by using CFD modeling for fire suppressions. J. Loss Prev. Process. Ind. 44, 626–632.
Welker, J.R., Sliepcevich, C.M., 1966. Bending of wind-blown flames from liquid pools. Fire Technol. 2, 127–135.
Yi, H., Feng, Y., Wang, Q., 2019. Computational fluid dynamics (CFD) study of heat radiation from large liquefied petroleum gas (LPG) pool fires. J. Loss Prev. Process. Ind. 61, 262–274.
Zabetakis, M.G., Burgess, D.S., 1961. Research on Hazards Associated with Production and Handling of Liquid Hydrogen. Bureau of Mines, Washington, D.C [Fire hazards and formation of shock-sensitive condensed mixtures].
Zukoski, E.E., 1995. Combustion Fundamentals of Fire. Academic Press, London.